Mechanics of Advanced Composite Structures 6 (2019) 81 – 94

Mechanics of Advanced Composite Structures

journal homepage: http://MACS.journals.semnan.ac.ir

Semnan University

Transient Thermal Stresses Analysis in a FPGM Cylinder

N. Habibi [a*], S. Samawati [b], O. Ahmadi [c]

[a] *Mechanical Engineering Department, University of Kurdistan, Sanandaj, 66177-15175, Iran,*
[b] *Mechanical Engineering Department, Khajeh Nasir Toosi University of Technology, Tehran, Iran,*
[c] *Mechanical Engineering Department, Urmia University, Urmia, Iran*

PAPER INFO

Paper history:
Received 2018-05-29
Received in revised form 2018-07-22
Accepted 2019-04-25

Keywords:
Piezo-electric
FGPM
Hollow cylinder
Transient
Thermal Stress

ABSTRACT

The present study aims to investigate the analysis of stress, strain, displacement, and electrical potential of a thick hollow cylinder made of FGPM under mechanical and thermal loads. Distribution of mechanical property of material is considered along the shell stick through the power distribution function. Thermal loads have been taken to signify the difference of temperature between outer and inner surfaces for each type of mechanical property. After extracting and solving the differential equations in transient state and the observation of mechanical and thermal boundary conditions, governing functions are obtained through the following parameters: thermal conduction non-homogeneous parameters, thermal linear distribution coefficient, elastic stiffness constant, piezo-electric coefficient, and dielectric constants.

1. Introduction

The cylinders are widely used under applied loads and in recent years, they have experienced the emergence of governing equations on cylinders and methods sought to solve such equations. Jabbari et al. [1] investigated the effect of transient state thermal stress on a FGPM cylinder. They used direct method to solve the problem and compared the results with the results of the power function method.

The presented method is very extensible even to solve the mixed boundary condition problems. They studied the distribution of stress in cylinder for different boundary conditions. Jabbari et al. [2] in another research investigated the effect of mechanical and transient state thermal stresses in FGM cylinder analytically through the Bessel functions. The analysis shows that as the power law indices increase, the mechanical stresses increased as well until they reach a constant value, where the mechanical stresses remain constant from the metal surface to the ceramic surface of the cylinder; this value of mechanical effective stress yields the optimum pressure vessel. Soufiye's study [3] scrutinized FGM cone cylindrical shell under widespread pressed loads and press of hydrostatic, where some formulas were obtained. Ging-Hua Zhang et al. [4] surveyed the thermo-dynamical behavior and the effects of type and load on one FGM, applying Van Karmen Theory (VKT) through numerical solution method under the change of the surface shape. Hui-Shen et al. [5] investigated the post-buckling FGM hybrid shells under pressed loads in thermal hoops; then, they analyzed the post-buckling for an FGM

* Corresponding author. Tel.: +98-87-33660072; Fax: +98-87-33668513
E-mail address: n.habibi@uok.ac.ir

DOI: 10.22075/macs.2019.14988.1147

piezoelectric cylindrical shell under hydrostatic pressure and electrical load in thermal hoops. Shao [6] presented three-dimensional solution to obtain the stress fields in an FGM cylindrical plate with a finite length; mechanical and thermal loads were tested on the plate and the results were presented in graphs.

Piezoelectric materials show coupled effects between elastic and electric fields; these materials have been widely used as the actuators or sensors in smart composite material systems. Many analytical studies concerning piezo-elastic or piezo-thermo-elastic problems have been reported and the results have been published in book forms [7]. Recently, a new type of piezoelectric material named functionally graded piezoelectric materials (FGPM), with material constants varying continuously in terms of thickness direction has been developed [8-10]. Electromagneto-thermoelastic treatment for a FGPM hollow cylinder has been measured [11]. Obata et al. [12] presented the solution for thermal stresses of a hollow thick cylinder made of FGM under 2D transient temperature distribution. Shariyat et al. [13] presented the nonlinear transient thermal stress and elastic wave propagation analyses of thick temperature-dependent FGM cylinders, through a second-order point-collocation method. Lü Chen et al. [14] investigated the elastic mechanical behavior of Nano-scaled FGM films incorporating surface energies. Afsar et al. [15] studied the inverse problems of material distributions for prescribed apparent fracture toughness in FGM coatings around a circular hole in infinite elastic media. Farid et al. [16] investigated the 3D temperature dependent free vibration analysis of FGM curved panels resting on two-parameter elastic foundation using a hybrid semi-analytic, differential quadrature method. Bagri and Eslami [17] showed the general coupled thermo-elasticity of FGM annular disk, considering the Lord–Shulman Theory. Samsam et al. [18] studied the buckling of thick FG plates under mechanical and thermal loads. Jabbari et al. [19] studied an axisymmetric mechanical and thermal stresses in thick, short length FGM cylinder. They applied separation of variables and Complex Fourier series to solve the heat conduction and Navier equation. Thieme et al. [20] presented the Titanium powder sintering for the preparation of a porous FGM destined as a skeletal replacement implant. Jabbari et al. [21] used the generalized Bessel function to investigate the axisymmetric mechanical and thermal stresses in thick short length FGM cylinders. Asghari and Ghafoori [22] investigated the 3D elasticity solution for functionally graded rotating disks. Khoshgoftar et al. [23] presented the thermo-elastic analysis of a thick walled FGPM cylinder.

Jabbari et al. [24] investigated the transient solution of asymmetric mechanical and thermal stresses for hollow cylinders made of functionally graded material. They analytically obtained the temperature distribution, as function of radial and circumferential directions and time, using the the method of separation of variables and generalized Bessel function, and a direct method were used to solve the Navier equations, using the Euler equation and complex Fourier series. The difference between reference [24] and the present work is in cylindermaterial, which at present work is used piezo-electric material in FGM cylinder.

In another research [25], an analytical method of a thermoelastic problem for a medium with FG material properties was developed in a theoretical manner for the elliptic-cylindrical coordinate system subjected to the presumption that the material properties except for Poisson's ratio and density are assumed to vary arbitrarily with the exponential law in the radial direction. The Stress Functions Extraction in a hollow cylinder under heating and cooling was investigated by Lamba et al. [26].

Thermal elastic stress distribution occurred on FGM long hollow cylinders was analytically defined under thermal, mechanical and thermo-mechanical loads. In the closed form, solutions for elastic stresses and displacements are obtained analytically using the infinitesimal deformation theory of elasticity [27].

Khobragade et al. [28-36] investigated the temperature distribution, displacement function, and stresses of a thin as well as thick hollow cylinder and also have established the displacement function, temperature distribution and stresses of a semi-infinite cylinder. In addition, Cursun et al. [37], has performed an elastic stress analysis of annular FGMs discs under both uniform pressures on the inner surface and a linearly decreasing temperature distribution.

The study of temperature distribution and thermal stresses of a FG thick hollow cylinder with temperature-dependent material properties by Manthena and Kedar [38] was investigated. All the material properties except Poisson’s ratio are assumed to be dependent on temperature and spatial coordinate z. The two-dimensional transient heat conduction equation was solved under convective heat transfer condition with varying point heat source.

The application of this structure is mostly in military structures, aerospace, and also the medical engineering. The main difference between this article and other similar studies is in the solution method and how to achieve the answer. In addition, in similar previous studies, more than FGM was used while FPGM was used in this work.

2. Equilibrium Equations

The main objective of the present study is surveying a hollow thick FGPM cylinder with inner and outer radii, *a* and *b*, which are shown in Fig. 1. The condition is in transient state; therefore, the component of time is observed in temperature equations.

This picture is the designed FGM Cylinder model in ABAQUS and aims to show a general schema. Strain–displacement equations are as follow:

$$\varepsilon_{rr} = u_{,r} \ , \varepsilon_{\theta\theta} = \frac{u}{r} + \frac{1}{r} v_{,\theta} \ , \varepsilon_{r\theta} = \frac{1}{2}\left(\frac{1}{r} u_{,\theta} + v_{,r} - \frac{v}{r}\right) \tag{1}$$

where u and v are the displacement components along r and θ directions, respectively. The stress-strain equations could be expressed as follow [24]:

$$\sigma_{rr} = C_{11}\varepsilon_{rr} + C_{12}\varepsilon_{\theta\theta} + e_{21}E_r - z_r T(r,\theta) \tag{2-1}$$

$$\sigma_{\theta\theta} = C_{22}\varepsilon_{\theta\theta} + C_{12}\varepsilon_{rr} + e_{22}E_r - z_\theta T(r,\theta) \tag{2-2}$$

$$\sigma_{r\theta} = 2C_{44}\varepsilon_{r\theta} - e_{24}E_\theta \tag{2-3}$$

The material used for this sample is orthotropic.

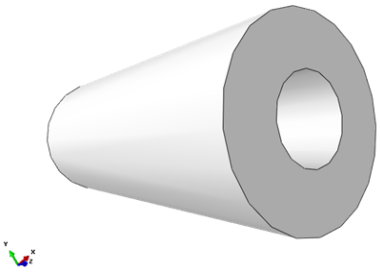

Fig. 1. Schematic view of a FGPM cylinder

where:

$$z_r = C_{11}\alpha_r + 2C_{12}\alpha_\theta \ , z_\theta = C_{22}\alpha_\theta + 2C_{12}\alpha_r \tag{3}$$

In the above relationship, coefficients C_{ij}, e_{ij}, ε_{ii}, g_{ij} (i=1,2), are the constants of elastic, piezoelectric, dielectric and temperature coefficient.

Furthermore, C_{ij}, e_{ij} (i, j = 1, 2, 4) are elastic, piezoelectric constants. Also, Z_r, Z_θ; the material parameters, (E_r, E_θ); the electric potential, T(r,θ); temperature distribution and α_r, α_θ are thermal expansion coefficients, respectively. And governing equations on potential electrical field are [24]:

$$D_{rr} = e_{21}\varepsilon_{\theta\theta} + e_{21}\varepsilon_{rr} - \chi_{11}E_r + g_{22}T(r,\theta) \tag{4-1}$$

$$D_{\theta\theta} = 2e_{24}\varepsilon_{r\theta} - \chi_{22}E_\theta + g_{21}T(r,\theta) \tag{4-2}$$

$$E_r = \frac{\partial\varphi}{\partial r} \ , \quad E_r = \frac{1}{r}\frac{\partial\varphi}{\partial\theta} \tag{4-3}$$

Here, C_{ij}, e_{ij} and χ_{ii} are elastic, piezoelectric, and dielectric constants, g_{ij} (i=1, 2) signify the thermal coefficients. In addition, electro-static and equilibrium equations are as follow:

$$\sigma_{rr,r} + \frac{1}{r}\sigma_{r\theta,\theta} + \frac{1}{r}(\sigma_{rr} - \sigma_{\theta\theta}) = 0 \tag{5-1}$$

$$\sigma_{r\theta,r} + \frac{1}{r}\sigma_{\theta\theta,\theta} + \frac{2}{r}\sigma_{r\theta} = 0 \tag{5-2}$$

$$\frac{\partial}{\partial r}(D_{rr}) + \frac{1}{r}D_{rr} + \frac{1}{r}\frac{\partial}{\partial\theta}(D_{\theta\theta}) = 0 \tag{5-3}$$

Using weight-power equations, the modelling of nonhomogeneous property can be defined as follow [24]:

$$e_{ij} = \bar{e}_{ij}r^m, g_{2i} = \bar{g}_{2i}r^{2m}, z_{r,\theta} = \bar{z}_{r,\theta}r^{2m}$$
$$\chi_{ii} = \bar{\chi}_{ii}r^m, \alpha_r = \alpha_{01}r^m, \alpha_\theta = \alpha_{02}r^m \tag{6}$$

where $\bar{e}_{ij}, \bar{g}_{2i}, \bar{z}_{r,\theta}, \bar{\chi}_{ii}, \alpha_{01}, \alpha_{02}$ are the material parameters and m is the power-low indices of the material. The equilibrium equations are obtained as follow in terms of the displacement components:

$$u_{,rr} + (m+1)\frac{1}{r}u_{,r} + \frac{1}{r^2}\left(\frac{C_{12}(m+1)-C_{22}}{C_{33}}\right)u + \frac{1}{r^2}\frac{C_{44}}{C_{11}}u_{,\theta\theta} + \frac{1}{r}\left(\frac{C_{12}}{C_{11}} + \frac{C_{44}}{C_{11}}\right)(v_{,\theta})_{,r} + \frac{1}{r^2}\left(\frac{mC_{12}-C_{22}-C_{44}}{C_{11}}\right)(v_{,\theta})r^m = \left(\left(\frac{(m_1+m_4-1)C_{11}-2C_{12}}{C_{11}}r^{m-1}\alpha_{01} + \frac{(2m_2+m_4+1)C_{12}+C_{22}}{C_{11}}r^{m-1}\alpha_{02}\right)T(r,\theta) + \frac{C_{11}r^m\alpha_{01}+2C_{12}r^m\alpha_{02}}{C_{11}}\frac{dT}{dr}\right)r^m \tag{7}$$

$$(C_{44}v_{,rr} + (m+1)C_{44}\frac{1}{r}v_{,r} + \frac{1}{r^2}C_{22}v_{,\theta\theta} - \frac{1}{r^2}(m+1)C_{44}v + \frac{1}{r}(C_{44} + C_{12})u_{,r\theta} + (\frac{1}{r^2}\big((m+1)C_{44} + C_{12}\big)u_{,\theta})r^m ((2C_{12}r^m\alpha_{01} + C_{22}r^m\alpha_{02})\frac{1}{r}T_{,r})r^m \quad (8)$$

$$u_{,rr} + \left(m + \frac{\bar{e}_{21}}{\bar{e}_{11}}\right)\frac{1}{r}u_{,r} + \frac{1}{2r^2}\frac{\bar{e}_{24}}{\bar{e}_{11}}u_{,\theta\theta} + \frac{m}{r^2}\frac{\bar{e}_{21}}{\bar{e}_{11}}u + \frac{1}{r}\left(\frac{2\bar{e}_{21} + \bar{e}_{24}}{2\bar{e}_{11}}\right)v_{,r\theta} - \frac{1}{r^2}\frac{\bar{e}_{24}}{\bar{e}_{11}}v_{,\theta} - \left(\frac{\eta_{11}}{\bar{e}_{11}}\varphi_{,rr} + \left(\frac{\eta_{11}}{\bar{e}_{11}}\right)\frac{1}{r}\varphi_{,r} + \frac{1}{r^2}\left(\frac{\eta_{22}}{\bar{e}_{11}}\right)\varphi_{,\theta\theta}\right)r^{-m} = -r^{-m}(\left((2m+1)\frac{\bar{e}_{22}}{\bar{e}_{11}}\right)T + \frac{\bar{e}_{22}}{\bar{e}_{11}}T_{,r} + \frac{\bar{e}_{21}}{\bar{e}_{11}}T_{,\theta}) \quad (9)$$

where:

$$S = \frac{g_{21}}{g_{22}} \quad , \quad f = \frac{z_\theta}{z_r} \quad (10)$$

In the next section, first temperature distribution is obtained in transient state for cylinder, the application of which will solve the differential equations.

2.1. Temperature Distribution

It is assumed that in hollow cylinder, T_a and T_b represent the temperatures in internal and external radii, respectively. Therefore, heat conduction equation for cylindrical coordinates will be as follows:

$$\frac{1}{r^2}\frac{\partial}{\partial r}\left(kr^2\frac{\partial T}{\partial r}\right) + \frac{1}{r^2}\frac{\partial}{\partial\theta}\left(k\frac{\partial T}{\partial\theta}\right) + \frac{\partial}{\partial z}\left(k\frac{\partial T}{\partial z}\right) + R = \rho c\frac{\partial T}{\partial t} \quad (11)$$

where, R is the inner thermal source, k is the coefficient of thermal conduction, ρ is density and c is the specific heat capacity, the components depending on the property of cylindrical source are as follow:

$$k(r) = k_0 r^m \,, \rho = \rho_0 r^m \,, c = c_0 r^m \,, k_0 = \frac{k(a)}{a^m} \quad (12)$$

where k_0, ρ_0, c_0 the material parameters and m are is the power-low indices of the material. Substituting Eq. (12) into Eq. (11), heat conduction equation in FGM cylinder can yield the following equation:

$$T_{,rr} + \frac{1}{r}(m+1)T_{,r} + \frac{1}{r^2}T_{,\theta\theta} + \frac{R}{k_0 r^m} = \frac{\rho_0 c_0}{k_0}\, r^m T_{,t} \quad (13)$$

Initial and boundary conditions are shown as:

$$T(r,\theta,0) = g_3(r,\theta) \,, x_{11}T(b,\theta,t) + x_{12}T_{,r}(b,\theta,t) = g_1(\theta,t) \,, x_{21}T(a,\theta,t) + x_{22}T_{,r}(a,\theta,t) = g_2(\theta,t) \quad (14)$$

The solution of heat conduction equation (11) is assumed to be:

$$T(r,\theta,t) = w(r,\theta,t) + Y(r,\theta,t) \quad (15)$$

$w(r,\theta,t)$ is defined in such a way that the boundary conditions for $Y(r,\theta,t)$ are zero Such that the definition of $w(r,\theta,t)$ guarantees the vanishing of boundary conditions for $Y(r,\theta,t)$:

$$W(r,\theta,t) = A(\theta,t)r^2 + B(\theta,t)r \quad (16)$$

A and B are the unknown functions obtained from Eqs. [37] and [38]. Therefore:

$$r^m Y_{,t} - \frac{k_0}{\rho_0 c_0}\left(Y_{,rr} + \frac{1}{r}(m+1)Y_{,r} + \frac{1}{r^2}Y_{,\theta\theta}\right) = R_1 \quad (17)$$

$$R_1 = \frac{R}{\rho c} - A_{,t}r^2 - B_{,t}r + \frac{k}{\rho c}(4A + A_{,\theta\theta} + \frac{1}{r}(B + B_{,\theta\theta}) \quad (18)$$

$$x_{11}Y(b,\theta,t)+x_{12}Y_{,r}(b,\theta,t)=0\,,\quad x_{21}Y(a,\theta,t)+x_{22}Y_{,r}(a,\theta,t)=0\,,Y(r,\theta,0)=g_3(r,\theta)-w(r,\theta,0) \tag{19}$$

To solve the Eq. (17), using the method of separation of variables, onecan write:

$$Y(r,\theta,t)=\sum_{n=-\infty}^{\infty}\sum_{k=-\infty}^{\infty}F_{kn}(r)G_{kn}(t)e^{in\theta} \tag{20}$$

In addition, *i* is a complex number. where:

$$\begin{aligned}&F_{kn}(r)\\&=r^{-\frac{k+1}{2}}\left(a_1J_p\left(\lambda_{kn}\frac{r^f}{f}\right)+a_2J_{-p}\left(\lambda_{kn}\frac{r^f}{f}\right)\right)\\&=r^{-\frac{k+1}{2}}C_p\left(\lambda_{kn}\frac{r^f}{f}\right)C_p\left(\lambda_{kn}\frac{r^f}{f}\right)\\&=a_1J_p\left(\lambda_{kn}\frac{r^f}{f}\right)+a_2J_{-p}\left(\lambda_{kn}\frac{r^f}{f}\right),f\\&=\frac{k+2}{2}\end{aligned} \tag{21}$$

$J_p$and J_{-p} are the Bessel function of the first kind:

$$J_p\left(\lambda_{kn}\frac{r^f}{f}\right)=\sum_{l=0}^{\infty}\frac{(-1)^k\left(\frac{\lambda_{kn}}{2}\frac{r^f}{f}\right)^{2l+p}}{l!\,\Gamma(l+p+1)} \tag{22-1}$$

$$J_{-p}\left(\lambda_{kn}\frac{r^f}{f}\right)=\sum_{l=0}^{\infty}\frac{(-1)^k\left(\frac{\lambda_{kn}}{2}\frac{r^f}{f}\right)^{2l-p}}{l!\,\Gamma(l+p+1)} \tag{22-2}$$

On the other hand, substituting equation (20) in relation (17), equation (23) can be obtained:

$$\frac{\rho_0c_0}{k_0}\frac{\dot{G}_{kn}(t)}{G_{kn}}=\frac{\ddot{F}_{kn}(t)+\frac{k+1}{2}\dot{F}_{kn}(t)-\frac{n^2}{r^2}F_{kn}}{F_{kn}}=-\lambda_{kn}^2 \tag{23}$$

. (Dot) is time derivative, ″ is displacement derivative. By using (20):

$$Y(r,\theta,t)=\sum_{n=-\infty}^{\infty}\sum_{k=1}^{\infty}r^{-\frac{k+1}{2}}a_1C_p\left(\lambda_{kn}\frac{r^f}{f}\right)G_{kn}(t)e^{in\theta} \tag{24}$$

$$x_{11}Y(b,\theta,t)+x_{12}Y_{,r}(b,\theta,t)=0\,,\quad x_{21}Y(a,\theta,t)+x_{22}Y_{,r}(a,\theta,t)=0 \tag{25}$$

Substituting (20) in previous relations (15, 17&19) gives the following system of differential equations:

$$\begin{aligned}&a_1(x_{11}r^{-\frac{k+1}{2}}J_p(\lambda_{kn}\frac{b^f}{f})-\frac{k+1}{2}x_{12}r^{-\frac{k+3}{2}}J_p(\lambda_{kn}\frac{b^f}{f})+x_{12}r^{-\frac{k+1}{2}}\dot{J}_p(\lambda_{kn}\frac{b^f}{f}))\\&+a_2(x_{11}J_{-p}(\lambda_{kn}\frac{b^f}{f})+x_{12}J_{-p}(\lambda_{kn}\frac{b^f}{f})+x_{12}r^{-\frac{k+1}{2}}\dot{J}_{-p}(\lambda_{kn}\frac{b^f}{f}))=0\end{aligned} \tag{26-1}$$

$$\begin{aligned}&a_1(x_{11}r^{-\frac{k+1}{2}}J_p(\lambda_{kn}\frac{b^f}{f})-\frac{k+1}{2}x_{12}r^{-\frac{k+3}{2}}J_pa_1(x_{11}r^{-\frac{k+1}{2}}J_p(\lambda_{kn}\frac{a^f}{f})-\frac{k+1}{2}x_{12}r^{-\frac{k+3}{2}}J_p(\lambda_{kn}\frac{a^f}{f})+x_{12}r^{-\frac{k+1}{2}}\dot{J}_p(\lambda_{kn}\frac{a^f}{f}))\\&+a_2(x_{11}J_{-p}(\lambda_{kn}\frac{a^f}{f})+x_{12}J_{-p}(\lambda_{kn}\frac{a^f}{f})+x_{12}r^{-\frac{k+1}{2}}\dot{J}_{-p}(\lambda_{kn}\frac{a^f}{f}))=0\end{aligned} \tag{26-2}$$

By putting the obtained determinant of coefficients in this differential equation, equal to zero the positive roots λ_{kn}will emerge as follow:

$$\begin{aligned}&\left(x_{11}r^{-\frac{k+1}{2}}J_p(\lambda_{kn}\frac{b^f}{f})-\frac{k+1}{2}x_{12}r^{-\frac{k+3}{2}}J_p(\lambda_{kn}\frac{b^f}{f})+x_{12}r^{-\frac{k+1}{2}}\dot{J}_p(\lambda_{kn}\frac{b^f}{f})\right)\left(x_{11}J_{-p}(\lambda_{kn}\frac{a^f}{f})+x_{12}J_{-p}(\lambda_{kn}\frac{a^f}{f})+x_{12}r^{-\frac{k+1}{2}}\dot{J}_{-p}(\lambda_{kn}\frac{a^f}{f})\right)\\&-\left(x_{11}r^{-\frac{k+1}{2}}J_p(\lambda_{kn}\frac{a^f}{f})-\frac{k+1}{2}x_{12}r^{-\frac{k+3}{2}}J_p(\lambda_{kn}\frac{a^f}{f})+x_{12}r^{-\frac{k+1}{2}}\dot{J}_p(\lambda_{kn}\frac{a^f}{f})\right)\left(x_{11}J_{-p}(\lambda_{kn}\frac{b^f}{f})+x_{12}J_{-p}(\lambda_{kn}\frac{b^f}{f})+x_{12}r^{-\frac{k+1}{2}}\dot{J}_{-p}(\lambda_{kn}\frac{b^f}{f})\right)=0\end{aligned} \tag{27}$$

Substituting Eq (24) into Eq (17) gives:

$$R_1 = \sum_{n=-\infty}^{\infty}\sum_{k=1}^{\infty} r^{-\frac{k+1}{2}} a_1 C_p(\lambda_{kn}\frac{r^f}{f})(\dot{G}_{kn}(t) + \frac{k_0}{\rho_0 c_0}\lambda_{kn}^2 G_{kn}(t))e^{in\theta} \quad (28)$$

where the following relation is extracted:

$$\dot{G}_{kn}(t) + \frac{k}{\rho c}\lambda_{kn}^2 G_{kn}(t) = \frac{2n+1}{2\pi\left|C_p(\lambda_{kn}\frac{r^f}{f}\right|^2 a_1} \times \int_0^{2\pi}\int_a^b r^{\frac{k+3}{2}} R_1(r,\theta,t) C_p(\lambda_{kn} r)\, e^{-in\theta} dr d\theta \quad (29)$$

The previous equation is an ordinary differential equation which will be solved through the application of:

$$\left|C_p(\lambda_{kn}\frac{r^f}{f}\right|^2 = \int_a^b [C_p(\lambda_{kn}\frac{r^f}{f}]^2 r dr\,,\ \ R_1^*(t) = \int_0^{2\pi}\int_a^b r^{\frac{k+3}{2}} R_1(r,\theta,t) C_p(\lambda_{kn}\frac{r^f}{f})\, e^{-in\theta} dr d\theta \quad (30)$$

The solution of the differential equation (31) is as follows:

$$G_{kn}(t) = e^{-\int \pi dt}(b_{1n} + \int \frac{2n+1}{2\left|C_p(\lambda_{kn}\frac{r^f}{f}\right|^2 a_1} R_1^*(t) e^{-\int \pi dt}\mathrm{dt}) \quad (31)$$

where:

$$\tau = \frac{k_0}{\rho_0 c_0}\lambda_{kn}^2 \quad (32)$$

therefore:

$$Y(r,\theta,t) = \sum_{n=-\infty}^{\infty}\sum_{k=1}^{\infty} r^{-\frac{k+1}{2}} a_1 C_p(\lambda_{kn}\frac{r^f}{f}) e^{-\int \pi dt}(b_{1n} + \int \frac{2n+1}{2\left|C_p(\lambda_{kn}\frac{r^f}{f}\right|^2 a_1} R_1^*(t) e^{-\int \pi dt}\mathrm{dt}) e^{in\theta} \quad (33)$$

Using the initial condition, indeed, equation (17) gives:

$$Y(r,\theta,0) = g_3(\theta,r) - w(r,\theta,0) \quad (34)$$

So, the equilibrium equation is extracted as follows:

$$(r,\theta,t) = \sum_{n=-\infty}^{\infty}\sum_{k=1}^{\infty} r^{-\frac{k+1}{2}} a_1 C_p(\lambda_{kn}\frac{r^f}{f}) e^{-\int \pi dt}(b_{1n} + \int \frac{2n+1}{2\left|C_p(\lambda_{kn}\frac{r^f}{f}\right|^2 a_1} R_1^*(t) e^{-\int \pi dt}\mathrm{dt}) e^{in\theta} + A(t,\theta) r^2 + B(t,\theta)\, r \quad (35)$$

where:

$$b_{1n} = \frac{2n+1}{2\left|C_p(\lambda_{kn}\frac{r^f}{f}\right|^2} \times \int_0^{2\pi}\int_a^b r^{\frac{k+3}{2}} (g_3(r,\theta) - w(r,\theta,0)) C_p(\lambda_{kn}\frac{r^f}{f})\, e^{-in\theta} dr d\theta - G(0) \quad (36)$$

A and B as unknown functions are obtained by solving the following 2-equations and 2-unknown system:

$$x_{11}T(b,\theta,t) + x_{12}T_{,r}(b,\theta,t) = g_1(\theta,t)\,,\quad x_{21}T(a,\theta,t) + x_{22}T_{,r}(a,\theta,t) = g_2(\theta,t) \quad (37)$$

$$A(\theta,t)(x_{11}b^2 + 2x_{12}b) + B(\theta,t)(x_{11}b + x_{12}) = g_1(\theta,t)\,,\quad A(\theta,t)(x_{21}a^2 + 2x_{22}a) + B(\theta,t)(x_{21}a + x_{22}) = g_2(\theta,t) \quad (38)$$

2.2. Equilibrium Equations Solution

Equations (7), (8), and (9) could be solved using the power series as follow [24]:

$$u(r,\theta) = \sum_{n=-\infty}^{\infty} u_n(r)e^{in\theta}, v(r,\theta) = \sum_{n=-\infty}^{\infty} v_n(r)e^{in\theta}, \varphi(r,\theta) = \sum_{n=-\infty}^{\infty} \varphi_n(r)e^{in\theta} \quad (39)$$

By substituting (36) and (31) into (7), (8) and (9):

$$\begin{aligned}
&\ddot{u}_n(r) + (k+1)\frac{1}{r}\dot{u}_n(r) \\
&+ \frac{1}{r^2}\left(\frac{C_{12}(k+1) - C_{22} - n^2C_{44}}{C_{11}}\right)u_n(r) \\
&+ \frac{1}{r}\left(in\left(\frac{C_{11}+C_{44}}{C_{11}}\right)\right)\dot{v}_n(r) \\
&+ \frac{in}{r^2}\left(\frac{kC_{12} - C_{22} - C_{66}}{C_{11}}\right)v_n(r) \\
&= \left(\left(\frac{(k_1+k_4-1)C_{11} - 2C_{12}}{C_{11}}r^{k-1}\alpha_{01}\right.\right. \\
&\left.\left. + \frac{2(k_2+k_4+1)C_{12} + C_{22}}{C_{11}}r^{k-1}\alpha_{02}\right)\right. \\
&\left.\times T(r,\theta) \right. \\
&\left. + \frac{C_{11}r^k\alpha_{01} + 2C_{12}r^k\alpha_{02}}{C_{11}}\frac{dT}{dr}\right)r^k
\end{aligned} \quad (40)$$

$$\begin{aligned}
&\ddot{v}_n(r) + (k+1)\frac{1}{r}\dot{v}_n(r) - \frac{1}{r^2}((k+1) \\
&\quad + \frac{n^2C_{22}}{C_{44}})v_n(r) - \frac{in}{r}(1 \\
&\quad + \frac{C_{12}}{C_{44}})\dot{u}_n(r) \\
&\quad - \frac{in}{r^2}\left(k+1\right. \\
&\quad \left. + \frac{C_{12}}{C_{44}}\right)u_n(r) \\
&\quad = ((2C_{12}r^k\alpha_{01} \\
&\quad + C_{22}r^k\alpha_{02})\frac{1}{r}\frac{dT}{dr})r^k
\end{aligned} \quad (41)$$

$$\begin{aligned}
&\ddot{u}_n(r) + \left(k + \frac{\bar{e}_{21}}{\bar{e}_{11}}\right)\frac{1}{r}\dot{u}_n(r) - \\
&\frac{1}{r^2}\frac{2k\bar{e}_{21} - n^2\bar{e}_{24}}{2\bar{e}_{11}}u_n(r) + \\
&\frac{in}{r}\left(\frac{2\bar{e}_{21}+\bar{e}_{24}}{2\bar{e}_{11}}\right)\dot{v}_n(r) - \frac{in}{r^2}\frac{\bar{e}_{24}}{\bar{e}_{11}}v_n(r) - \\
&\frac{\bar{\chi}_{22}}{\bar{e}_{11}}\ddot{\varphi}_n(r) - \frac{\bar{\chi}_{22}}{\bar{e}_{11}} \times \frac{1}{r}(k+2)\dot{\varphi}_n(r) + \\
&\frac{n^2}{r^2}\frac{\bar{\chi}_{11}}{\bar{e}_{11}}\varphi_n(r) = -r^{m-1}(((2k+1)\frac{\bar{g}_{22}}{\bar{e}_{11}})T + \\
&\frac{\bar{g}_{22}}{\bar{e}_{11}}T_{,r} + \frac{\bar{g}_{21}}{\bar{e}_{11}}T_{,\theta})
\end{aligned} \quad (42)$$

Solution of homogeneous part of three upper equations is as follow:

$$u_n^g(r) = Dr^n, v_n^g(r) = Er^n, \varphi_n^g(r) = Fr^n \quad (43)$$

where D, E and F are constants obtained using boundary conditions and g means the general solution, through substituting (43) into (42), (41) and (40):

$$\left[\eta(\eta-1) + (k+1)\eta + \frac{C_{12}(k+1) - C_{22} - n^2C_{44}}{\bar{C}_{11}}\right]D + i\left[\left(\frac{C_{12}+C_{44}}{C_{11}}\right)\eta + \frac{kC_{12} - C_{22} - C_{44}}{C_{11}}\right]nE = 0 \quad (44)$$

$$\left[\eta(\eta-1) + (k-1)\eta - ((k+1) + \frac{n^2C_{22}}{C_{44}}\right]E + i\left[\left(\frac{C_{12}+C_{44}}{C_{44}}\right)\eta + (k+1 + \frac{C_{12}}{C_{44}})\right]nD = 0 \quad (45)$$

$$\begin{aligned}
&\left[\eta(\eta-1) + \left(k + \frac{\bar{e}_{21}}{\bar{e}_{11}}\right)\eta + (\frac{2k\bar{e}_{21} - n^2\bar{e}_{24}}{2\bar{e}_{11}})\right]D + in\left[\left(\frac{2\bar{e}_{21}+\bar{e}_{24}}{2\bar{e}_{11}}\right)\eta - \frac{\bar{e}_{24}}{\bar{e}_{11}}\right]E - \left[\frac{\bar{\chi}_{22}}{\bar{e}_{22}}\eta(\eta-1) + \frac{\bar{\chi}_{22}}{\bar{e}_{22}}\eta(k+2) - n^2\frac{\bar{\chi}_{11}}{\bar{e}_{11}}\right]F = 0
\end{aligned} \quad (46)$$

In order to provide the evident solution, the above equations must be equal to zero. Therefore, Eigen vectors μ are as follow:

$$\begin{aligned}
&\left[\eta(\eta-1) + \eta(k+1) + \frac{C_{12}(k+1) - C_{22} - n^2C_{44}}{C_{11}}\right] \times \left[\eta(\eta-1) + \eta(k-1) - ((k+1) + n^2\frac{C_{22}}{C_{44}})\right] \times \\
&\left(-\left[(\frac{\bar{\chi}_{22}}{\bar{e}_{22}})\eta(\eta-1) + (\frac{\bar{\chi}_{22}}{\bar{e}_{22}})\eta(k+2) - n^2(\frac{\bar{\chi}_{11}}{\bar{e}_{11}})\right]\right) - \left[\left(\frac{C_{12}+C_{44}}{C_{11}}\right)\eta + \left(\frac{C_{12}k - C_{22} - C_{44}}{C_{11}}\right)\right]n \times \left[\left(1 + \frac{C_{12}}{C_{44}}\right)\eta + \left(k + 1 + \frac{C_{12}}{C_{44}}\right)\right]n \times \left[\frac{\bar{\chi}_{22}}{\bar{e}_{22}}\eta(\eta-1) + (\frac{\bar{\chi}_{22}}{\bar{e}_{22}})\eta(k+2) - n^2(\frac{\bar{\chi}_{11}}{\bar{e}_{11}})\right] = 0
\end{aligned} \quad (47)$$

where, η_{nj} is the more general case for η,Also, η as a parameter in equation (43), only one case n is used, Whereas, it is observed in equation (39) that displacements are a set of special cases for $n =$

$-\infty$ to $n=\infty$; therefore, for determining the general solution, η_{nj} is used. Consequently, the general solution is the linear combination of eigen vectors as follows:

$$u_n^g(r)=\sum_{j=1}^{6} D_{nj}^g r^{\eta_{nj}},\ v_n^g(r)=\sum_{j=1}^{6} N_{nj}D_{nj}^g r^{\eta_{nj}},\ \varphi_n^g(r)=\sum_{j=1}^{6} M_{nj}D_{nj}^g r^{\eta_{nj}} \tag{48}$$

where, by applying (47), $M_{nj}$and $N_{nj}$are obtained. Particular solution is assumed as follows [24]:

$$u_{kn}^p = r^{\frac{m+1}{2}}\sum_{l=1}^{\infty}\left(D_{knl1}^p J_p\left(\lambda_{kn}\frac{r^f}{f}\right) + D_{knl2}^p J_{-p}\left(\lambda_{kn}\frac{r^f}{f}\right)\right)\times Q_{kn}(t) + D_{knl3}^p r^{k+2} + D_{knl4}^p r^{k+3} \tag{49-1}$$

$$v_{kn}^p = r^{\frac{k+1}{2}}\sum_{l=1}^{\infty}\left(D_{knl5}^p J_p\left(\lambda_{kn}\frac{r^f}{f}\right) + D_{knl6}^p J_{-p}\left(\lambda_{kn}\frac{r^f}{f}\right)\right)\times Q_{kn}(t) + D_{knl7}^p r^{k+2} + D_{knl8}^p r^{k+3} \tag{49-2}$$

$$\varphi_{kn}^p = r^{\frac{k+1}{2}}\sum_{l=1}^{\infty}\left(D_{knl9}^p J_p\left(\lambda_{kn}\frac{r^f}{f}\right) + D_{knl10}^p J_{-p}\left(\lambda_{kn}\frac{r^f}{f}\right)\right)\times Q_{kn}(t) + D_{knl11}^p r^{k+2} + D_{knl12}^p r^{k+3} \tag{49-3}$$

By substituting upper equations and their derivations in (40), (41) and (42) and definition of Bessel function of the first kind and the value of temperature distribution, four 3-equations and 3-unknowns systems would be resulted .The coefficients D are obtained by solving four systems as follow:

$$\begin{cases} D_{kn1}^p x_{n1} + D_{kn5}^p x_{n2} + D_{kn9}^p x_{n3} = x_{n4} \\ D_{kn1}^p x_{n15} + D_{kn5}^p x_{n16} + D_{kn9}^p x_{n17} = x_{n18} \\ D_{kn1}^p x_{n29} + D_{kn5}^p x_{n30} + D_{kn9}^p x_{n31} = x_{n32} \end{cases} \tag{50-1}$$

$$\begin{cases} D_{kn2}^p x_{n5} + D_{kn6}^p x_{n6} + D_{kn10}^p x_{n7} = x_{n8} \\ D_{kn2}^p x_{n19} + D_{kn6}^p x_{n20} + D_{kn10}^p x_{n21} = x_{n22} \\ D_{kn2}^p x_{n33} + D_{kn6}^p x_{n34} + D_{kn10}^p x_{n35} = x_{n36} \end{cases} \tag{50-2}$$

$$\begin{cases} D_{kn3}^p x_{n9} + D_{kn7}^p x_{n10} + D_{kn11}^p x_{n11} = 0 \\ D_{kn3}^p x_{n23} + D_{kn7}^p x_{n24} + D_{kn11}^p x_{n25} = 0 \\ D_{kn3}^p x_{n37} + D_{kn7}^p x_{n38} + D_{kn11}^p x_{n39} = 0 \end{cases} \tag{50-3}$$

$$\begin{cases} D_{kn4}^p x_{n12} + D_{kn8}^p x_{n13} + D_{kn12}^p x_{n14} = 0 \\ D_{kn4}^p x_{n26} + D_{kn8}^p x_{n27} + D_{kn12}^p x_{n28} = 0 \\ D_{kn4}^p x_{n40} + D_{kn8}^p x_{n41} + D_{kn12}^p x_{n42} = 0 \end{cases} \tag{50-4}$$

In the last two 2-equations and 2-unknown systems, since coefficients determinant matrix does not vanish, the possible solution of these systems is the evident solution. Solutions of first 2 systems yield other coefficients. Complete solution of displacement is as follows:

$$u_{kn}(r,t) = r^{\frac{k+1}{2}}\sum_{l=0}^{\infty}\left(D_{knl1} J_p\left(\lambda_{kn}\frac{r^f}{f}\right) + D_{knl2} J_{-p}\left(\lambda_{kn}\frac{r^f}{f}\right)\right)\times Q_{kn}(t) + D_{kn3} r^{k+2} D_{knl4} r^{k+3} + \sum_{j=1}^{6} B_{nj} r^{\eta_{nj}} \tag{51-1}$$

$$v_{kn}(r,t) = r^{\frac{k+1}{2}}\sum_{l=0}^{\infty}\left(D_{knl5} J_p\left(\lambda_{kn}\frac{r^f}{f}\right) + D_{knl6} J_{-p}\left(\lambda_{kn}\frac{r^f}{f}\right)\right)\times Q_{kn}(t) + D_{kn7} r^{k+2} D_{kn8} r^{k+3} + \sum_{j=1}^{6} N_{nj} B_{nj} r^{\eta_{nj}} \tag{51-2}$$

$$\varphi_{kn}(r,t) = r^{\frac{k+1}{2}}\sum_{l=0}^{\infty}\left(D_{knl9} J_p\left(\lambda_{kn}\frac{r^f}{f}\right) + D_{knl10} J_{-p}\left(\lambda_{kn}\frac{r^f}{f}\right)\right)\times Q_{kn}(t) + D_{kn11} r^{k+2} D_{kn12} r^{k+3} + \sum_{j=1}^{6} M_{nj} B_{nj} r^{\eta_{nj}} \tag{51-3}$$

For n = 0, the system of Navier equations would lead to the following single differential equation:

$$\ddot{u}_0(r) + (k+1)\frac{1}{r}\dot{u}_0(r) + \frac{1}{r^2}\left(\frac{C_{12}(k+1)-C_{22}-n^2C_{44}}{C_{11}}\right)u_0(r) = \tag{52}$$

$$\begin{aligned}&(\Big(\tfrac{(k_1+k_4-1)C_{11}-2C_{12}}{C_{11}}r^{k-1}\alpha_{01}+\\&\tfrac{2(k_2+k_4+1)C_{12}+C_{22}}{C_{11}}r^{k-1}\alpha_{02}\Big)\times T(r,\theta)+\\&\tfrac{C_{11}r^k\alpha_{01}+2C_{12}r^k\alpha_{02}}{C_{11}}\tfrac{dT}{dr})r^k\\&\ddot{u}_0(r)+\Big(k+\tfrac{\bar{e}_{21}}{\bar{e}_{11}}\Big)\tfrac{1}{r}\dot{u}_0(r)-\\&\tfrac{1}{r^2}\tfrac{2k\bar{e}_{21}-n^2\bar{e}_{24}}{2\bar{e}_{11}}u_0(r)-\tfrac{\bar{\chi}_{22}}{\bar{e}_{11}}\ddot{\varphi}_0(r)-\tfrac{\bar{\chi}_{22}}{\bar{e}_{11}}\times\\&\tfrac{1}{r}(k+2)\dot{\varphi}_0(r)+\tfrac{n^2}{r^2}\tfrac{\bar{\chi}_{11}}{\bar{e}_{11}}\varphi_0(r)=\\&-r^{k-1}(((2\mathrm{k}+1)\tfrac{\bar{g}_{22}}{\bar{e}_{11}})T+\tfrac{\bar{g}_{22}}{\bar{e}_{11}}T_{,r}+\tfrac{\bar{g}_{21}}{\bar{e}_{11}}T_{,\theta})\end{aligned}\tag{53}$$

The upper differential equations are Euler differential equations, where it could be assumed that the solution of the homogeneous part is as follows:

$$u_0^g(r)=D_0r^{\eta_0}\,,\varphi_0^g(r)=F_0r^{\eta_0}\tag{54}$$

WhereB_0, D_0 and μ_0 are obtained using boundary conditions. Substituting the upper equation in homogeneous part of Eqs (52) and (53) would give the following result:

$$\begin{aligned}&(\eta_0^2+(k+1)\eta_0\\&+\left(\left(\frac{C_{12}(k+1)-C_{22}-n^2C_{44}}{\bar{C}_{11}}\right)\right)D_0=\end{aligned}\tag{55-1}$$

$$\begin{aligned}&(\eta_0(\eta_0-1)(k+\frac{\bar{e}_{21}}{\bar{e}_{11}})\eta_0\\&+(\frac{2k\bar{e}_{21}-n^2\bar{e}_{24}}{2\bar{e}_{11}}))D_0\\&-(\frac{\bar{\chi}_{22}}{\bar{e}_{11}}\eta_0(\eta_0-1)\\&+(\frac{(k+2)\bar{\chi}_{22}}{\bar{e}_{11}})\eta_0\\&-n^2\frac{\bar{\chi}_{11}}{\bar{e}_{11}})F_0=0\end{aligned}\tag{55-2}$$

In order to obtain the non-trivial solution of the above equation, the determinant of coefficients of constants *B, C* and *D* must vanish, which leads to the evaluation of the eigenvector η, as presented in the following equation:

$$\begin{aligned}&(\eta_0^2+(k+1)\eta_0+\\&(\tfrac{C_{12}(k+1)-C_{22}-n^2C_{44}}{\bar{C}_{11}}))\times((\tfrac{\bar{\chi}_{22}}{\bar{e}_{11}}\eta_0(\eta_0-\\&1)+(\tfrac{(k+2)\bar{\chi}_{22}}{\bar{e}_{11}})\eta_0-n^2\tfrac{\bar{\chi}_{11}}{\bar{e}_{11}}))=0\end{aligned}\tag{56}$$

Thus, the general solution, utilizing the linearity lemma, is a linear combination of all values of eigenvalues, which is obtained from:

$$\begin{aligned}&u_0^g(r)=\textstyle\sum_{j=1}^4(D_{0j}r^{\eta_{0j}}\,,\varphi_0^g(r)=\\&\textstyle\sum_{j=1}^4M_{0j}D_{0j}r^{\eta_{0j}}\end{aligned}\tag{57}$$

The particular solution of Eqs. (52) and (53) is assumed as:

$$\begin{aligned}u_{k0}(r,t)=r^{\frac{k+1}{2}}\sum_{l=0}^{\infty}&(D_{k0l1}J_p\left(\lambda_{k0}\frac{r^f}{f}\right)\\&+D_{k0l2}J_{-p}\left(\lambda_{k0}\frac{r^f}{f}\right))\\&\times Q_{k0}(t)\\&+D_{k03}r^{k+2}D_{k04}r^{k+3}\end{aligned}\tag{58-1}$$

$$\begin{aligned}\varphi_{k0}(r,t)=r^{\frac{k+1}{2}}\sum_{l=0}^{\infty}&(D_{k0l9}J_p\left(\lambda_{k0}\frac{r^f}{f}\right)\\&+D_{k0l10}J_{-p}\left(\lambda_{k0}\frac{r^f}{f}\right))\\&\times Q_{k0}(t)\\&+D_{k011}r^{k+2}D_{k012}r^{k+3}\end{aligned}\tag{58-2}$$

By substituting the upper equations in (52) and (53), four 2-equations and 2-unknown systems would be found as follow, where by solving it, D will be derived:

$$\begin{cases}D_{k01}x_{n1}+D_{k09}x_{n2}=x_{n3}\\D_{k01}x_{n11}+D_{k09}x_{n12}=x_{n13}\end{cases}\tag{59-1}$$

$$\begin{cases}D_{k02}x_{n4}+D_{k010}x_{n5}=x_{n6}\\D_{k02}x_{n14}+D_{k010}x_{n15}=x_{n16}\end{cases}\tag{59-2}$$

$$\begin{cases}D_{k03}x_{n7}+D_{k011}x_{n8}=0\\D_{k03}x_{n17}+D_{k011}x_{n18}=0\end{cases}\tag{59-3}$$

$$\begin{cases}D_{k04}x_{n9}+D_{k012}x_{n10}=0\\D_{k04}x_{n19}+D_{k012}x_{n20}=0\end{cases}\tag{59-4}$$

In the Eq. (59), regarding the 2-equations and 2-unknown systems, since coefficient determinant matrix does not vanish, possible solution of these systems is the evident solution, and the solutions of first two-systems will yield other coefficients. Thus, the complete solution, using the Eqs. (52), (53) and (58) is:

$$\begin{aligned}&u(r,\theta)=r^{\frac{k+1}{2}}\textstyle\sum_{l=0}^{\infty}(D_{k0l1}J_p\left(\lambda_{k0}\frac{r^f}{f}\right)+\\&D_{k0l2}J_{-p}\left(\lambda_{k0}\frac{r^f}{f}\right))\times Q_{k0}(t)+\\&D_{k03}r^{k+2}D_{k0l4}r^{k+3}+\\&\textstyle\sum_{j=1}^6B_{nj}r^{\eta_{0j}}+\sum_{n=-\infty}^{\infty}(r^{\frac{k+1}{2}}\sum_{l=0}^{\infty}(D_{knl1}J_p\left(\lambda_{k}\right.\\&D_{knl2}J_{-p}\left(\lambda_{kn}\frac{r^f}{f}\right))\times Q_{kn}(t)+D_{kn3}r^{k+2}+\end{aligned}\tag{60-1}$$

$$D_{kn4}r^{k+3}+\sum_{j=1}^{6}B_{nj}r^{\eta_{nj}})e^{in\theta}$$

$$\begin{aligned}v(r,\theta)=\sum_{n=-\infty}^{\infty}(r^{\frac{k+1}{2}}\sum_{l=0}^{\infty}(D_{knl5}J_p\left(\lambda_{kn}\frac{r^f}{f}\right)\\+D_{knl6}^{p}J_{-p}\left(\lambda_{kn}\frac{r^f}{f}\right))\\\times Q_{kn}(t)+D_{knl7}r^{k+2}\\+D_{knl8}r^{k+3}\\+\sum_{j=1}^{6}N_{nj}B_{nj}r^{\eta_{nj}})e^{in\theta}\end{aligned}\quad(60\text{-}2)$$

$$\begin{aligned}&\varphi(r,\theta)\\&=r^{\frac{k+1}{2}}\sum_{l=0}^{\infty}(D_{k0l9}J_p\left(\lambda_{k0}\frac{r^f}{f}\right)\\&+D_{k0l10}J_{-p}\left(\lambda_{k0}\frac{r^f}{f}\right))\times Q_{k0}(t)\\&+D_{k011}r^{k+2}D_{k0l12}r^{k+3}\\&+\sum_{j=1}^{6}M_{0j}B_{0j}r^{\eta_{0j}}\\&+\sum_{n=-\infty}^{\infty}(r^{\frac{k+1}{2}}\sum_{l=0}^{\infty}(D_{knl9}J_p\left(\lambda_{kn}\frac{r^f}{f}\right)\\&+D_{knl10}J_{-p}\left(\lambda_{kn}\frac{r^f}{f}\right))\times Q_{kn}(t)\\&+D_{kn11}r^{k+2}+D_{kn12}r^{k+3}\\&+\sum_{j=1}^{6}M_{nj}B_{nj}r^{\eta_{nj}})\times e^{in\theta}\end{aligned}\quad(60\text{-}3)$$

The integration of the strain-displacement relationship given in Eq. (1) strains, and the results of Eq. (2), will yield the electrical field, radial, shear and hoop stresses, and the electrical displacements.

3. Results and Discussions

This section discusses the results of the analysis of FGPM transient state thermal of cylinders and compares the results with the stated references. In this part, the results obtained from this research are compared with the results of quoted references of [24] and [2]. The property of FGM and piezo are represented in Table 1. Inner radius is a=70 cm and outer radius is b=100 cm. Inner thermal source would be $R(r.\theta.t)=6\times10^{6}\times\frac{1}{r}\sin(t)\cos(2\theta)$.

Fig. 2 represents the thermal distribution related to radius and Fig. 3 shows the radial displacement in proportion to radius at θ = π/3; then, the obtained results were compared with the findings of [24] and [2] references. The boundary conditions are shown in Table 2.

The obtained results show good compatibility with the results of corresponding references in [24] and [2]. Maximum of difference between present work and the references [2] and [24] are shown in Table 3:

Table 1. The property of materials used in the analysis of transient state thermal of cylinders

FGM	piezoelectric	property
$C_{11}=13.9\times10^{10}$	$e_{11}=-5.2$	
$C_{12}=7.8\times10^{10}$	$e_{21}=-5.2$	Refs
$C_{13}=7.43\times10^{10}$	$e_{22}=15.1$	[24] , [2]
$C_{33}=11.5\times10^{10}$	$e_{25}=12.7$	
$C_{44}=2.56\times10^{10}$	g_{21}	
$\alpha_{01}=2.458\times10^{-6}$	$=-2.94\times10^{-6}$	
$\alpha_{02}=4.396\times10^{-6}$	g_{22}	
Metal:	$=-2.94\times10^{-6}$	
$k_0=18.1.\rho_0=4410$	χ_{11}	
$c_0=808.3$	$=64.64\times10^{-10}$	
Ceramic:	χ_{22}	
$k_0=2.036.$	$=56.22\times10^{-10}$	
$\rho_0=5600$		
$c_0=615.6$		

Table 2. The boundary conditions used in the analysis of transient state thermal of cylinders

electrical	boundary conditions	Thermal
	mechanical	
$\phi(a.\theta)=0$	$u(a.\theta)=0$	$g_1(\theta.t)=$
$\phi(b.\theta)$	$v(a.\theta)=0$	$20\sin(t)\cos(2\theta)$ ℃
$=30\cos(2\theta)$	$\sigma_{rr}(b.\theta)=0$	$g_2(\theta.t)=0$
$D_{rr}(a.\theta)=0$	$\sigma_{r\theta}(b.\theta)=0$	

Table 3. The comparison of temperature and radial displacement distributions along radius at θ = π/3

Parameter	Present work	Reference	Percentage of error
Temperature	50	46 [24]	8
Radial displacement	1.88	1.85 [2]	1

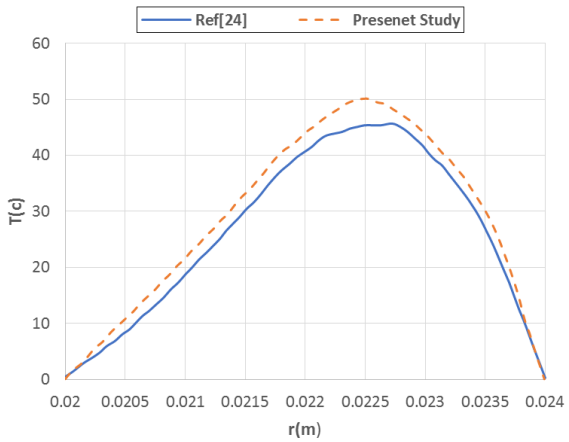

Fig. 2. The comparison of temperature distribution along radius at θ = π/3.

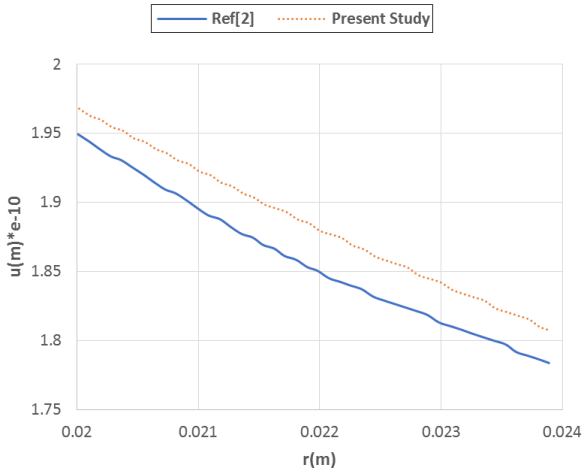

Fig. 3. The comparison of distribution of radial displacement along radius at θ = π/3.

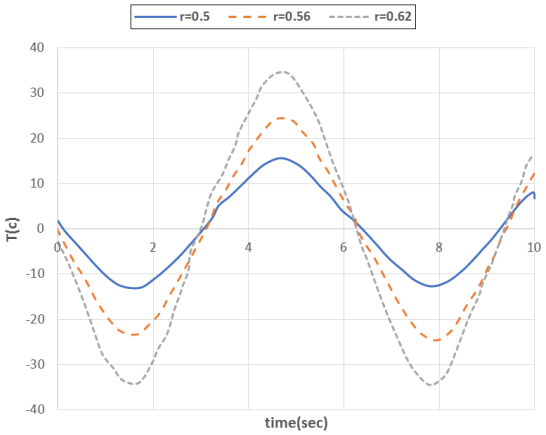

Fig. 4. Oscillation of the temperature with respect to the time at various radii

The following section, investigates the results of parametric and survey studies for the cylinders. Fig. 5 shows the radial displacement along radius at $= \frac{\pi}{3}$, for different values of m (indices in power-law). As the Fig. clearly shows, the increase of the radius would result in the reduction of radial displacement. Figs. 4, 6 and 7-10 show the oscillation of the temperature, radial displacement, hoop displacement, electrical potential, radial stress and shear stress with respect to the component of time at variation radii, respectively.

By increasing the radius, temperature increases and the domain of vibration gets larger. The value of radial displacement increases and the domain of vibration gets larger; also, the value of hoop displacement and electrical potential increase and the domain of vibration gets smaller. The value of radial stress and shear stress decrease and the domain of vibration gets smaller. Note that in the presented diagrams, the variations of parameters are dependent on the variation of m; i.e , when m increases temperature, radial displacement, electrical potential (except in outer surface where electrical potential equals the value of boundary conditions, zero), radial stress, and hoop stress decrease. According to the formerly stated points, when m gets larger, the resistance of FGM cylinder against thermal conduction increases. Also, the increase of m leads to the decrease of stress in source; thus, m is of paramount importance in the selection of the type of the material. Variation of m is effective on the variation of confidence coefficient.

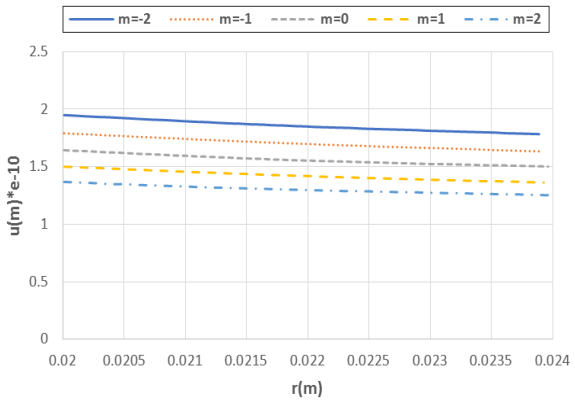

Fig. 5. The distribution of radial displacement along radius at θ = π/3.

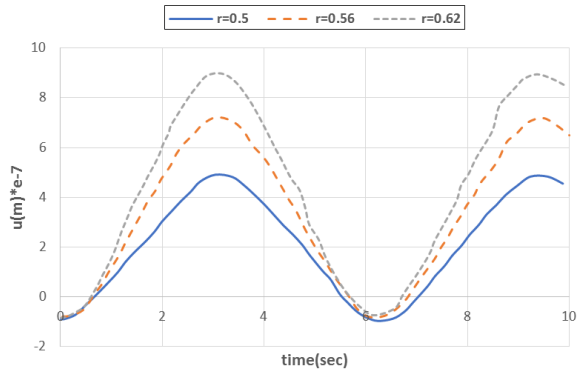

Fig. 6. Oscillation of the radial displacement with respect to the time at various radii.

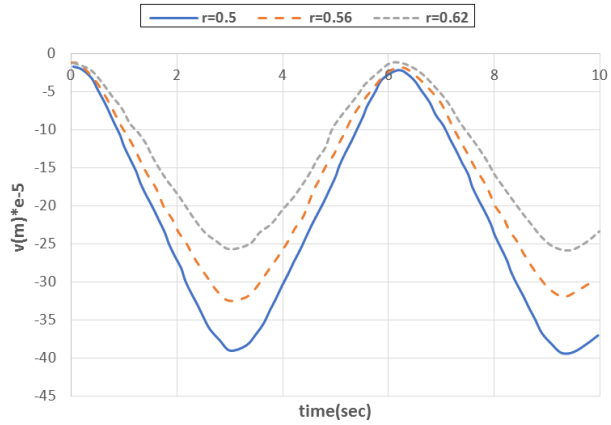

Fig. 7. Oscillation of the hoop displacement with respect to the time at various radii.

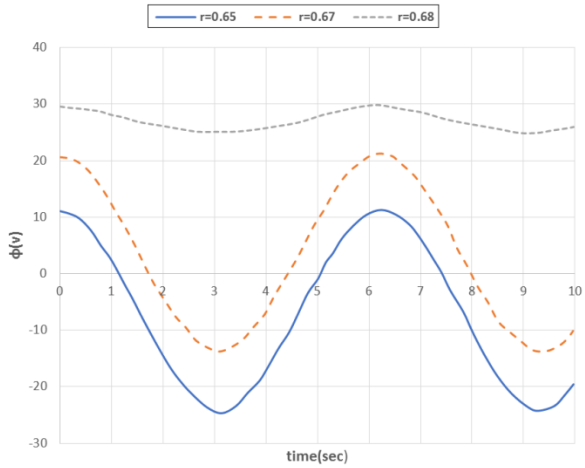

Fig. 8. Oscillation of the electrical potential with respect to the time at various radii.

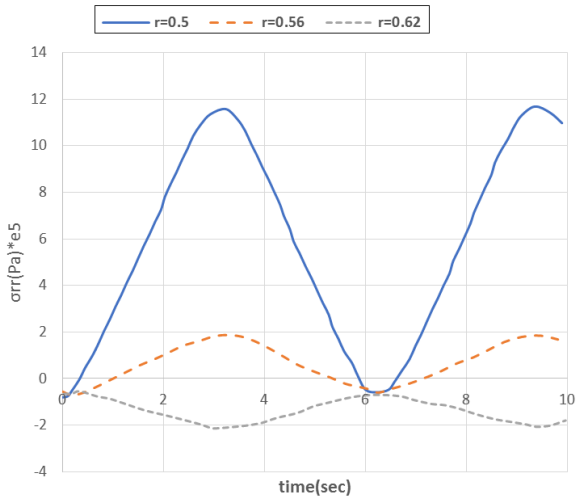

Fig. 9. Oscillation of the radial stress with respect to the time at various radii.

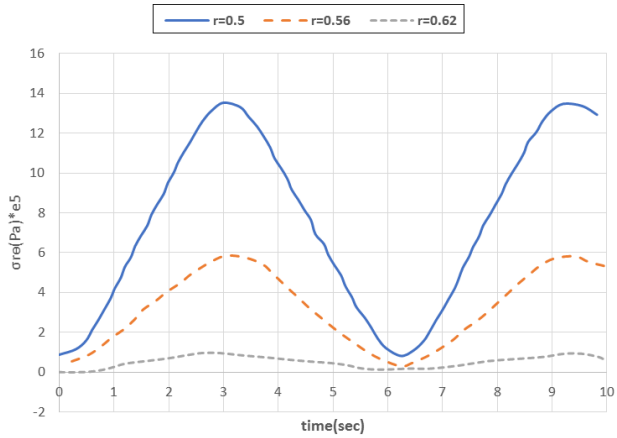

Fig. 10. Oscillation of the shear stress with respect to the time at various radii.

4. Conclusion

The results of the present study can be summarized as follow:

- By increasing the radius, the value of radial displacement and temperature increase and the domain of vibration gets larger. In addition, the value of hoop displacement and electrical potential increase and the value of radial and shear stresses decrease, and the domain of vibration gets smaller.
- Variable parameters of diagrams are dependent on the variations of m; when m increases, temperature, radial displacement, electrical potential (except in outer surface where electrical potential equals the value of boundary conditions, zero), radial and hoop stresses decrease.
- Increase of m leads to the reduction of stress in source; thus, m is of paramount importance in

the selection of the type of material. Variation of m is effective on the variation of confidence coefficient.

- Temperature, radial and hoop displacements, electrical potential, radial and shear stresses oscillate with respect to the component of time at various radii, respectively.

References

[1] Jabbari M, Sohrabpour S, Eslami MR, General Solution for mechanical and thermal stresses in a functionally graded hollow cylinder due to non-axisymmetric steady-state loads, *Journal of Applied Mechanics* 2003, 70;111-118.

[2] Jabbari M, Mohazzab, AH, One-Dimensional Moving Heat Source in a Hollow FGM Cylinder*, Journal of Pressure Vessel Technology* 2009; 131.

[3] Soufiye, AH, buckling analysis of FGM circular shells under combined loads and resting on the Pasternak type elastic foundation, 2011.

[4] Shi-Rong Li, Jing-Hua Zhang Yong-Gang, Zhao, Nonlinear Thermomechanical Post-Buckling of Circular FGM Plate with Geometric Imperfection, 2008.

[5] Hui-Shen, Shen Noda N, Post-buckling of pressure-loaded FGM hybrid-cylindrical shells in thermal environments, *Composite Structures* 2007; 77: 546 -560.

[6] Shao ZS, Wang TJ, Three-dimensional solutions for the stress fields in functionally graded cylindrical panel with finite length and subjected to thermal/mechanical loads. *Int J Solids Struct* 2006; 43: 3856–3874.

[7] Ding HJ, Chen, WQ, three dimensional problems of piezo-elasticity, Nova Science Publishers, New York, 2001.

[8] Wu, CCM, Kahn M, Moy W, Piezo-electric ceramics with functionally gradients: a new application in material design. *J Am Ceram Soc* 1996; 79: 809–812.

[9] Shelley WF, Wan S, Bowman KJ, functionally graded piezo-electric ceramics. *Mater Sci Forum* 1999; 308(311): 515-520.

[10] Zhu, XH, Zu J, Meng ZY, Zhu JM, Zhou SH Li Q, Micro displacement characteristics and microstructures of functionally graded piezoelectric ceramic actuator, *Mater Des* 2000; 21: 561–566.

[11] Dai HL, Hong L, Fu, YM, Xiao X, Analytical solution for electro magneto thermoelastic behaviors of a functionally graded piezoelectric hollow cylinder, *Appl Math Model* 2010; 34: 343–357.

[12] Obata Y, Kanayama K, Ohji T, Noda N, Two-Dimensional Unsteady Thermal Stresses in a Partially Heated Circular Cylinder Made of Functionally Graded Material, *Proceedings of Thermal Stresses, Pub. Branti Zew, Krakow, Poland* 1999; 595–598.

[13] Shariyat M, Lavasani SMH, Khaghani M, Transient thermal stress and elastic wave propagation analyses of thick temperature-dependent FGM cylinders, using a second-order point-collocation method, *Applied Mathematical Modelling* 2009,

[14] Lü CF, Chen WQ, Lim CW, Elastic mechanical behavior of Nano-scaled FGM films incorporating surface energies, *Composites Science and Technology* 2009; 69:1124-1130.

[15] Afsar AM, Sekine H, Inverse problems of material distributions for prescribed apparent fracture toughness in FGM coatings around a circular hole in infinite elastic media, *Composites Science and Technology* 2002; 62:1063-1077.

[16] Farid M, Zahedinejad P, Malekzadeh P, Three-dimensional temperature dependent free vibration analysis of functionally graded material curved panels resting on two-parameter elastic foundation using a hybrid semi-analytic, differential quadrature method, *Materials and Design* 2010; 31: 2-13.

[17] Bagri A, Eslami MR, generalized coupled thermos-elasticity of functionally graded annular disk considering the Lord–Shulman theory, *Composite Structures* 2008; 83: 168-179.

[18] Samsam Shariat, BA, Eslami, MR, buckling of thick functionally graded plates under mechanical and thermal loads, *Composite Structures* 2007; 78: 433–439.

[19] Jabbari M, Bahtui A, Eslami MR, Axisymmetric mechanical and thermal stresses in thick short length functionally graded material cylinder, *International Journal of Pressure Vessels and Piping* 2009; 86: 96-306.

[20] Thieme M, Wieters KP, Bergner F, Scharnweber D, Worch H, Ndop J, Kim TJ, Grill, Titanium powder sintering for preparation of a porous FGM Destined as a skeletal replacement implant, Materials Science Forum 1999; 308(311): 374-382.

[21] Jabbari M, Bahtui A, Eslami MR, Axisymmetric mechanical and thermal stresses in thick short length FGM cylinders, *Int. J. Press Vessel Pip* 2009; 86: 296–306.

[22] Asghari M, Ghafoori E, A three-dimensional elasticity solution for functionally graded ro-

tating disks, *Compos. Struct* 2010; 92: 1092-1099.

[23] Khoshgoftar MJ, Ghorbanpour Aranl A, Arefi A, Thermoelastic analysis of a thick walled cylinder made of functionally graded piezoelectric material, *Smart Mater. Struct* 2009; 18: 115007.

[24] Jabbari M, Vaghari AR, Exact solution for asymmetric transient thermal and mechanical stresses in FGM hollow cylinders with heat source, *Structural Engineering and Mechanics* 2008; 29 (5): 551-565.

[25] Manthena VR, Lamba NK, Kedar GD, Thermal stress analysis in a functionally graded hollow elliptic-cylinder subjected to uniform temperature distribution, *Applications and Applied Mathematics* 2017; 12 (1): 613-632.

[26] Lamba NK, Walde RT, Manthena VR. Khobragade NW, Stress Functions in a Hollow Cylinder under Heating and Cooling, *Journal of Statistics and Mathematics* 2012; 3(3): 118-124

[27] Kursun A, Kara E, Cetin E, Aksoy S, Kesimli A, Mechanical and Thermal Stresses in Functionally Graded Cylinders, World Academy of Science, *Engineering and Technology International Journal of Aerospace and Mechanical Engineering* 2014; 8(2): 303-308.

[28] Singru SS, Chauthale S, Khobragade NW, Thermal Stress Analysis of a Thick Hollow Cylinder, *International Journal of Engineering and Innovative Technology (IJEIT)* 2015; 5(3): 157-160.

[29] Walde Anjali RC, Pathak C, Khobragade NW, Thermal Stresses of a Solid Cylinder with Internal Heat Source, *Int. J. of Engg. And Information Technology* (2013); 3(1): 407-410.

[30] Jadhav CM, Khobragade NW, An Inverse Thermoelastic Problem of finite length thick hollow cylinder with internal heat sources, *Advances in Applied Science Research* (2013); 4(3): 302-314.

[31] Khobragade, NW, Thermal stresses of a hollow cylinder with radiation type conditions, *Int. J. of Engg. And Information Technology* (2013); 3(5): 25-32.

[32] Khobragade NW, Thermoelastic analysis of a solid circular cylinder, *Int. J. of Engg. And Information Technology* (2013): 3(5): 155-162.

[33] Khobragade NW, Thermoelastic analysis of a thick hollow cylinder with radiation conditions, *Int. J. of Engg. And Information Technology* (2013): 3(4): 380-387.

[34] Gahane TT, Khobragade NW, Transient Thermoelastic Problem of a Semi-infinite Cylinder with Heat Sources, *Journal of Statistics and Mathematics* (2012); 3(2): 87-93.

[35] Hiranwar PC, Khobragade NW, Thermoelastic Problem of a Cylinder with Internal Heat Sources, *Journal of Statistics and Mathematics* (2012); 3(2): 87-93.

[36] Khobragade NW, Khalsa L, Kulkarni A, Thermal Deflection of a Finite Length Hollow Cylinder due to Heat Generation, *Int. J. of Engg. And Information Technology* (2013); 3(1): 372-375.

[37] Kursun a, Topcu M, Tetik T, Stress Analysis of Functionally Graded Disc under Thermal and Mechanical Loads, *Physics Engineering*(2011); 10: 2949-2954.

[38] Manthena VR, Kedar GD, Transient thermal stress analysis of a functionally graded thick hollow cylinder with temperature-dependent material properties, *Journal of thermal stresses* (2018); 41(5): 568-582.